JOURNAL OF MATERIALS SCIENCE 27 (1992) 6213–6218

In situ reacted TiB_2-reinforced alumina

SHIH-CHENG CHUANG*, CHENG-TZU KUO
Institute of Mechanical Engineering, National Chiao-Tung University, Hsinchu, Taiwan 30050
CHI-TING HO, AI-KANG LI
Materials Research Laboratories, ITRI, Chutung, Hsinchu, Taiwan 31015

In situ formation of TiB_2 in Al_2O_3 matrix through the reaction of TiO_2, boron and carbon has been studied. In hot-pressed samples, in addition to TiB_2, TiC and Al_2TiO_5 were also found to be dispersed phases in Al_2O_3 matrix. However, in the case of pressureless-sintered samples, pure Al_2O_3/TiB_2 composite with $> 99\%$ relative density can be obtained through a preheating step held at 1300 °C for longer than 30 min and then sintering at a temperature above 1500 °C. Pressureless-sintered composite containing 20 vol% TiB_2 gives a flexural strength of 580 MPa and a fracture toughness of 7.2 MPa $m^{1/2}$.

1. Introduction

Alumina ceramics have attracted much attention for both electronic and structural applications; their low fracture toughness, however, is an obstacle to be overcome. Until now, making composites by adding various toughening agents such as whiskers [1] or particles [2–5] has been the most common way to toughen or strengthen alumina.

Using TiB_2 particles as a dispersed phase has been proved effective in strengthening alumina [4, 5]. Also, the high hardness (≈ 3300 kgf mm^{-2}) and good thermal conductivity (30 W m^{-1} $°C^{-1}$) of TiB_2 make the Al_2O_3/TiB_2 composite an excellent cutting tool material [6]. Basically the Al_2O_3/TiB_2 composite is not difficult to densify as a pressure is applied during sintering. The problem is the high reactivity of TiB_2 with moisture, which makes direct powder mixing difficult. In the present work, we used *in situ* formation of TiB_2 in an alumina matrix through the reaction of TiO_2, boron and carbon powders, which have no handling problems in an alumina matrix by hot-pressing or pressureless sintering. It was expected that the particle size of internally synthesized TiB_2 particles would be much finer than commercial powders. In addition to identifying the TiB_2 phase, the densification, microstructure evolution and the mechanical properties of this Al_2O_3/TiB_2 composite were investigated.

2. Experimental procedure

The starting materials used were Al_2O_3 powder (average particle size 0.3 μm, purity $> 99\%$), TiO_2 powder (average particle size 1.26 μm, purity $> 99\%$), boron powder (average particle size 1.3 μm) and carbon powder (average particle size 0.7 μm). The starting materials were mixed in a ball mill using ethanol as solvent. The mix ratio for TiO_2, boron and carbon was designed according to the stoichiometry of TiB_2. Before sintering, the mixed powders were die-pressed at a pressure of 20 MPa to form discs of 60 mm diameter and 5 mm thick. The discs were then placed in a graphite container and either hot pressed at a pressure of 30 MPa, or pressureless sintered under vacuum conditions. In the case of hot pressing, two firing patterns were used in the experiments, as shown in Fig. 1. In pattern A, the samples were directly heated up and hot-pressed at 1500 °C for 1 h. In pattern B, the samples were preheated at 1300 °C for 4 h before hot-pressing at 1500 °C for 1 h. Fig. 2 shows the pressureless-sintering profiles. Three firing patterns, designated C, D, E, were used in the experiment. In pattern C, the samples were directly pressureless sintered at 1300 °C (or 1500 °C) for 1 h at a heating rate of 30 °C min^{-1}. In pattern D, the samples were preheated at 1300 °C for 30 min and were then pressureless sintered at 1500 °C. In pattern E, the samples were preheated at 1300 °C for 0–4 h and then pressureless sintered at 1600 °C for 1 h.

The bulk density of the sintered body was determined by the Archimedes method. The samples were examined by using X-ray diffractometer (Philips APD170 Model) and optical microscope after being polished with diamond paste of particle size down to 1 μm. Thin foils for transmission electron microscopy (TEM) were prepared from thin slices cut using a low-speed diamond saw. These slices were then ground to a thickness of ~ 60–80 μm. The final thinning was carried out by ion-beam milling with a 5 kV argon-ion beam incident on both surfaces of the foil at an angle of 12°. Electron microscopy was performed using a scanning transmission electron microscope (Jeol 2000 FX).

The fracture toughness, K_{Ic}, was measured using the single-edge notched beam (SENB) method. Highly polished plates were cut into 3 mm × 4 mm × 5 mm

*Also with Materials Research Laboratories, ITRI, Chutung, Hsinchu, Taiwan 31015.

0022–2461 © *1992 Chapman & Hall*

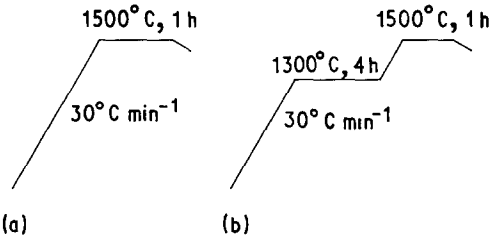

Figure 1 Firing patterns for hot-pressing in vacuum: (a) hot-pressing at 1500 °C for 1 h, pattern A; (b) preheating at 1300 °C for 4 h and then hot-pressing at 1500 °C for 1 h, pattern B.

bars and these were centre-notched to one-third of their thickness using a 0.15 mm thick diamond blade. The fracture strength, σ_f, was measured by the four-point bending method, following the JIS 1601 standard. Both flexural strength and fracture toughness were measured at room temperature in a testing machine operated at a constant crosshead speed of 0.5 mm min^{-1}.

3. Results and discussion

3.1. Sintering and phase identification

Fig. 3a shows the X-ray diffraction (XRD) pattern of the sintered body obtained by direct hot-pressing at 1500 °C for 1 h in vacuum without preheating (pattern A). Besides TiB_2 and TiC, Al_2TiO_5 phase was found in the Al_2O_3 matrix. If the samples were preheated at 1300 °C for 4 h and then hot pressed at 1500 °C for 1 h (pattern B, in argon), the XRD pattern was almost the same as Fig. 3a. However, if firing pattern B was adopted (but in vacuum), the peak intensity of TiB_2 was stronger, and those of TiC and Al_2TiO_5 were weaker, than if sintered in argon. This indicates that an argon atmosphere is not favourable for TiB_2 formation.

From the phases identified by XRD, the chemical reaction may be described by the following equation

$$2TiO_{2(s)} + 5C_{(s)} + 2B_{(s)} \rightarrow TiB_{2(s)} + TiC_{(s)} + 4CO_{(g)} \quad (1)$$

In this reaction the standard free energy change, ΔG^0, which is calculated based on JANAF thermochemical tables [7], is $-287.8\,kJ\,mol^{-1}$, indicating that the reaction is possible. However, in the case of hot-pressing, the CO gas cannot be freely released and this inhibits the previous reaction moving towards the right. Thus, the unreacted TiO_2 will react with Al_2O_3 to form Al_2TiO_5 phase [8] even at a temperature as low as 1000 °C. Therefore, hot-pressing is not favourable for obtaining pure Al_2O_3/TiB_2 composite.

To obtain Al_2O_3/TiB_2 composite without Al_2TiO_5, pressureless sintering was adopted. Fig. 4 shows the XRD patterns of the samples pressureless sintered using pattern C. It can be seen that a very small amount of Al_2TiO_5 still appeared when the samples were sintered at 1300 °C (Fig. 4a), while only TiB_2 and a trace amount of TiC were observed when the sintering temperature was raised to 1500 °C (Fig. 4b). This demonstrates that the Al_2TiO_5 phase can be eliminated by pressureless sintering at 1500 °C in vacuum.

3.2. Density

The density of the sintered body was measured after pressureless sintering. Fig. 5 shows the relative density as a function of sintering time at 1500 °C for the samples pressureless sintered by using pattern D; the relative densities of the composites increased with the sintering time. The composites containing 10 or 20 vol % TiB_2, can be densified up to 99% theoretical density if sintering time is longer than 3 h. On increasing the amount of synthesized TiB_2, the relative densities of the composites decrease drastically. For instance, the composite containing 30 vol % TiB_2 and sintered at 1500 °C for 4 h had a relative density of only 87% (Fig. 5), revealing that TiB_2 particles inhibit the densification of the composites.

Fig. 6 shows the dependence of relative density on preheating time at 1300 °C for samples pressureless sintered at 1600 °C for 1 h (pattern E). It is clearly seen that the composites containing 10 and 20 vol % TiB_2 can be fully densified after being preheated at 1300 °C for $\geqslant$ 2 h and then pressureless sintered at 1600 °C for 1 h in vacuum. It displays the same results as those sintered at 1500 °C for $\geqslant$ 3 h. This indicates that prolonging the preheating time at 1300 °C is crucial in the pumping out of the CO gas, because this gas is detrimental to densification of the composite. The final relative density of 96.3% for the composite containing 30 vol % TiB_2 can be obtained after being preheated at 1300 °C for 4 h and sintered at 1600 °C for 1 h in vacuum.

3.3. Microstructure investigation

Fig. 7 shows the optical micrograph of the sintered body containing 20 vol % TiB_2 which was preheated at 1300 °C for 30 min and then pressureless sintered

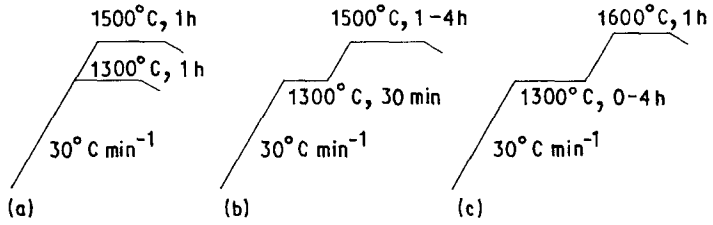

Figure 2 Firing patterns for pressureless-sintering in vacuum; (a) sintering at 1300 or 1500 °C for 1 h with a heating rate of 30 °C min^{-1}, pattern C; (b) preheating at 1300 °C for 30 min and then sintering at 1500 °C for 1–4 h, pattern D; (c) preheating at 1300 °C for 0–4 h and then sintering at 1600 °C for 1 h, pattern E.

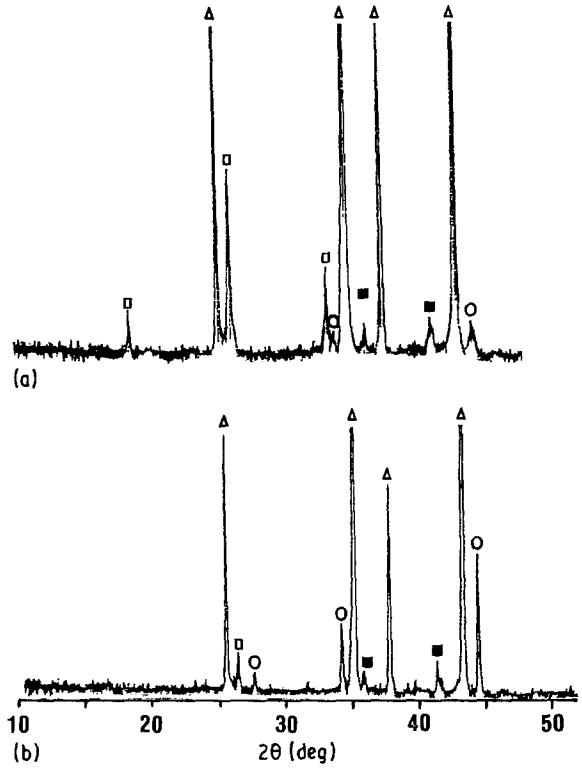

Figure 3 XRD patterns of the samples hot pressed using (a) firing pattern A, (b) firing pattern B. (△) Al_2O_3, (□) Al_2TiO_5, (○) TiB_2, (■) TiC.

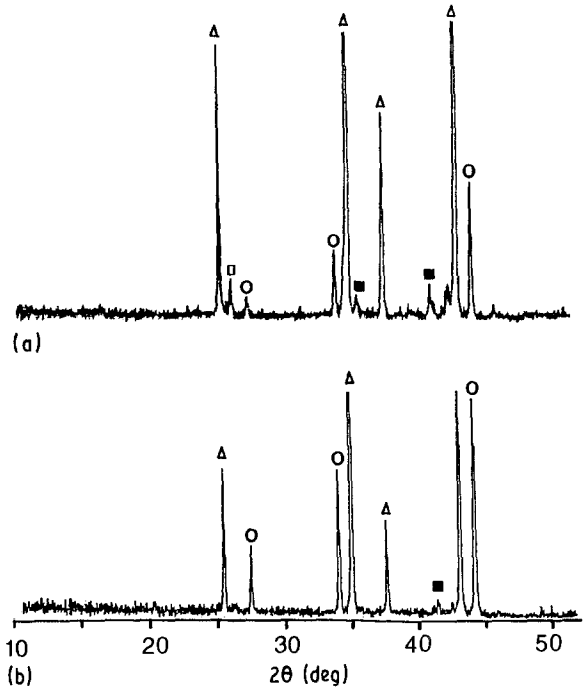

Figure 4 XRD patterns of the samples pressureless sintered by using firing pattern C at sintering temperatures: (a) 1300 °C; (b) 1500 °C. For key, see Fig. 3.

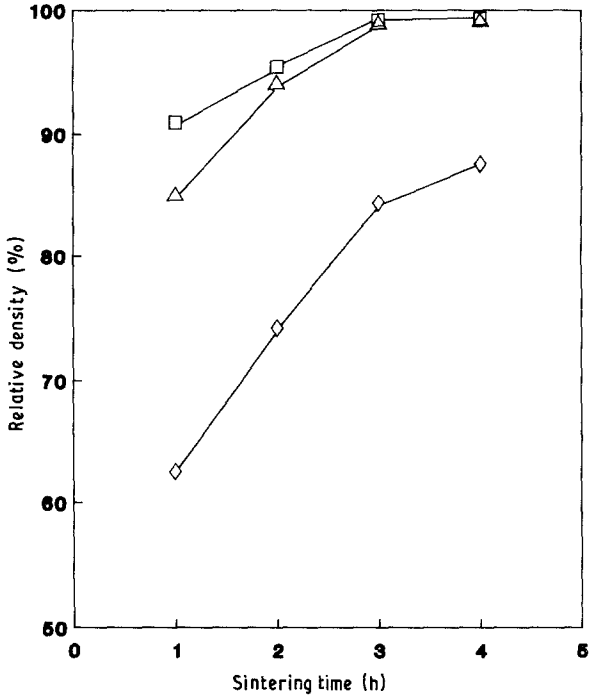

Figure 5 Relative densities of the composites as a function of sintering time at 1500 °C for 1–4 h on pressureless sintering (pattern D). (□) 10 vol %, (△) 20 vol %, (◇) 30 vol %.

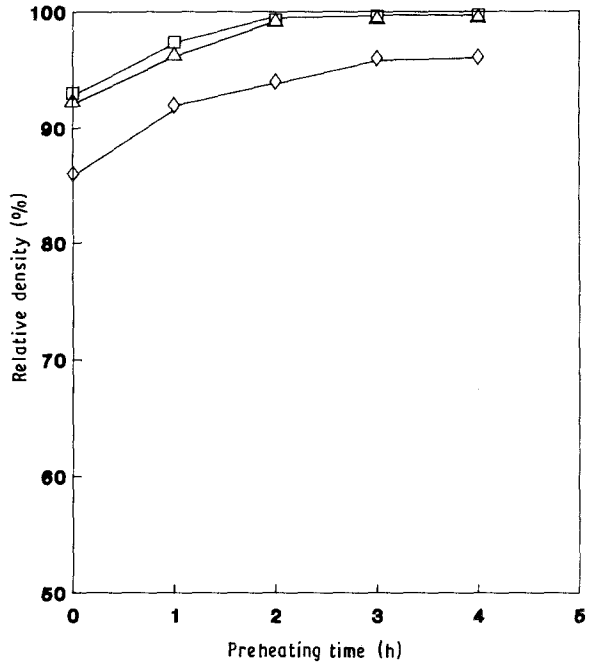

Figure 6 Relative densities of the composites as a function of preheating time at 1300 °C on pressureless sintering at 1600 °C for 1 h (pattern E). For key, see Fig. 5.

at 1500 °C for 2 and 3 h in vacuum, respectively. It appears that porosity decreases as the sintering time increases from 2 h to 3 h, which is consistent with the density measurements. As shown in Fig. 7b, the TiB_2 particles tend to coalesce as sintering time increases. For the specimen which was preheated at 1300 °C for $\geqslant$ 2 h and then sintered at 1600 °C for 1 h in vacuum, no coalescence of TiB_2 particles was observed, thus the TiB_2 particles remained fine and well dispersed throughout the Al_2O_3 matrix. A representative optical micrograph of the composite containing 10 vol % TiB_2, which was obtained through preheating at 1300 °C for 3 h and then sintering at 1600 °C for 1 h, is shown in Fig. 8. These results indicate that the microstructure of Al_2O_3/TiB_2 composite can be manipulated through the sintering profile. By lengthening the preheating time and raising the sintering temperature,

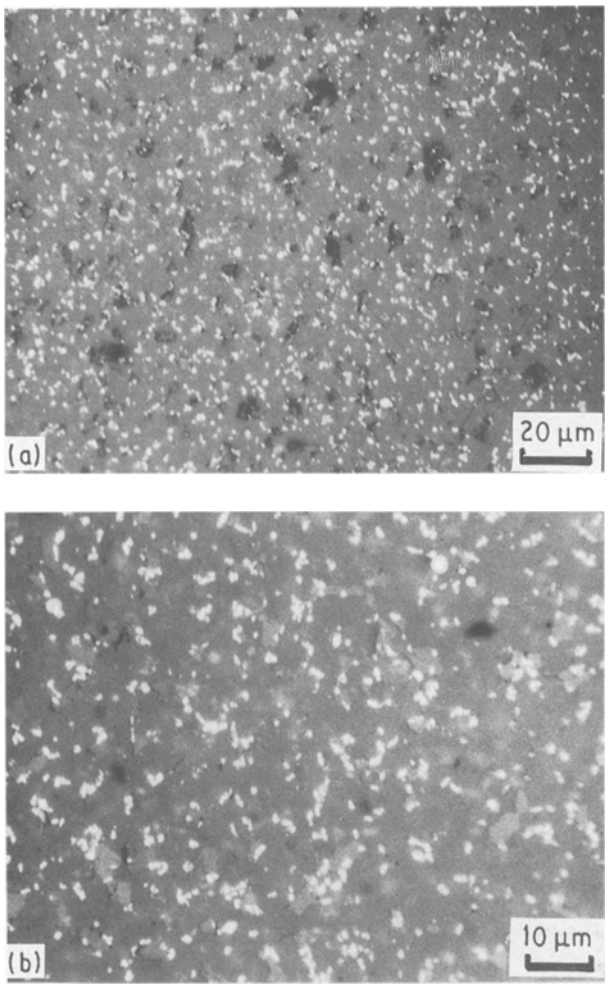

Figure 7 Optical micrograph of the composite containing 20 vol % TiB_2 obtained by preheating at 1300 °C for 30 min and then pressureless sintering at 1500 °C for (a) 2 h, (b) 3 h.

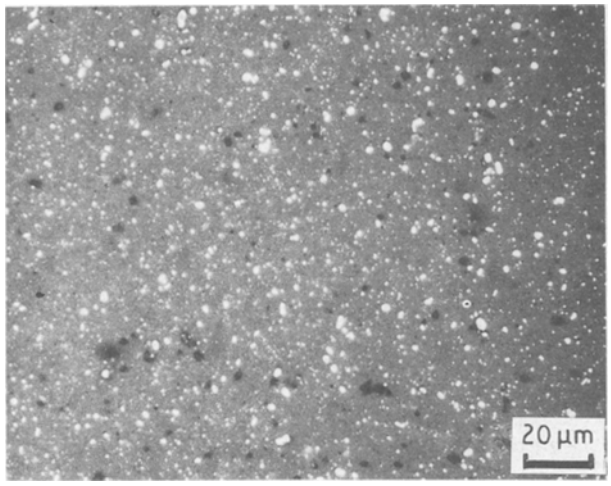

Figure 8 Optical micrograph of the composite containing 10 vol % TiB_2 obtained by preheating at 1300 °C for 3 h and then pressureless sintering at 1600 °C for 1 h.

fine-grain composites with better strength and toughness can be obtained.

Fig. 9a shows a typical transmission electron micrograph of the composite containing 20 vol % TiB_2 obtained by preheating at 1300 °C for 4 h and pressureless sintering at 1600 °C for 1 h in vacuum. It is

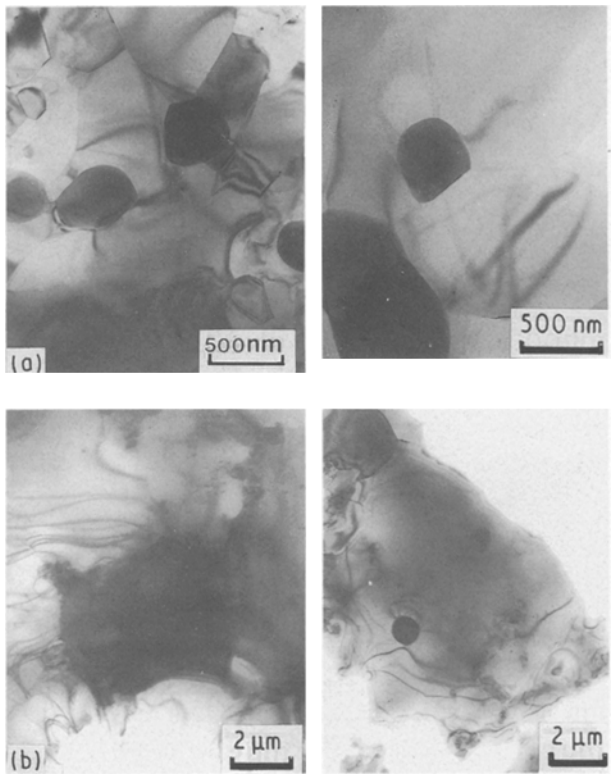

Figure 9 Transmission electron micrograph of the composite containing 20 vol % TiB_2 obtained by (a) preheating at 1300 °C up to 4 h and then pressureless sintering at 1600 °C for 1 h, (b) preheating at 1300 °C for 30 min and then pressureless sintering at 1500 °C for 4 h in vacuum.

estimated that the TiB_2 particle size ranges from 0.2–1.6 μm, much smaller than the commercially available powders, as expected. A large number of TiB_2 particles precipitated in the intragrains of the Al_2O_3 matrix, which induced the dislocation and strain contour in the surrounding matrix; some TiB_2 particles precipitated along the Al_2O_3 grain boundaries. In the case of Al_2O_3/20 vol % TiB_2 composite, which was obtained through preheating at 1300 °C for 30 min and then pressureless sintering at 1500 °C for 4 h in vacuum, the particle size of TiB_2 and the grain size of alumina were much larger than that sintered at 1600 °C for 1 h, as shown in Fig. 9b. This causes the deterioration of flexural strength as shown in Figs 10 and 11.

3.4. Mechanical properties

Fig. 10 shows the variation of flexural strength of the composites as a function of pressureless-sintering time and TiB_2 content, for which the composites were preheated at 1300 °C for 30 min and then sintered at 1500 °C. The flexural strength of the composite containing 20 vol % TiB_2, sintered at 1500 °C for longer than 3 h, was up to 520 MPa. Fig. 11 shows the flexural strength of the composites through preheating at 1300 °C for 2 or 3 h and then pressureless sintering at 1600 °C for 1 h. It can be seen that the flexural strength of the composite containing 20 vol % TiB_2 was up to 585 MPa as the preheating time was above 3 h. However, in the composite containing 30 vol %

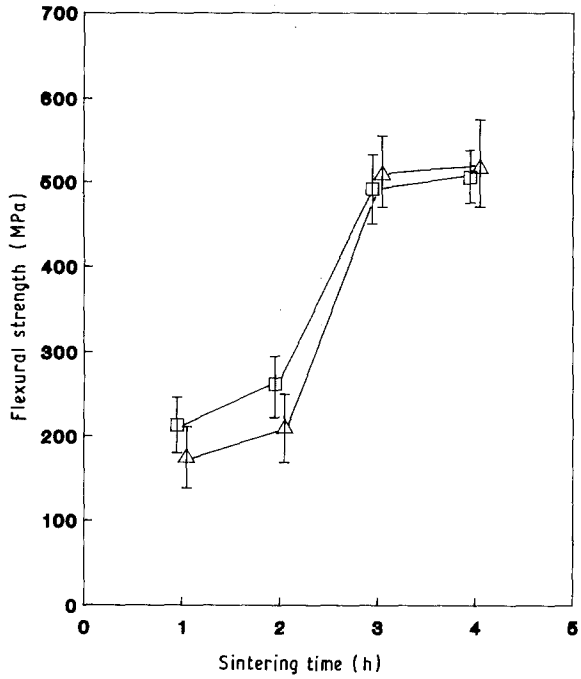

Figure 10 Variation of flexural strength of the composite containing (□) 10 and (△) 20 vol% TiB_2 as a function of pressureless-sintering time. The composites were obtained through preheating at 1300 °C for 30 min and then sintering at 1500 °C for 1–4 h in vacuum.

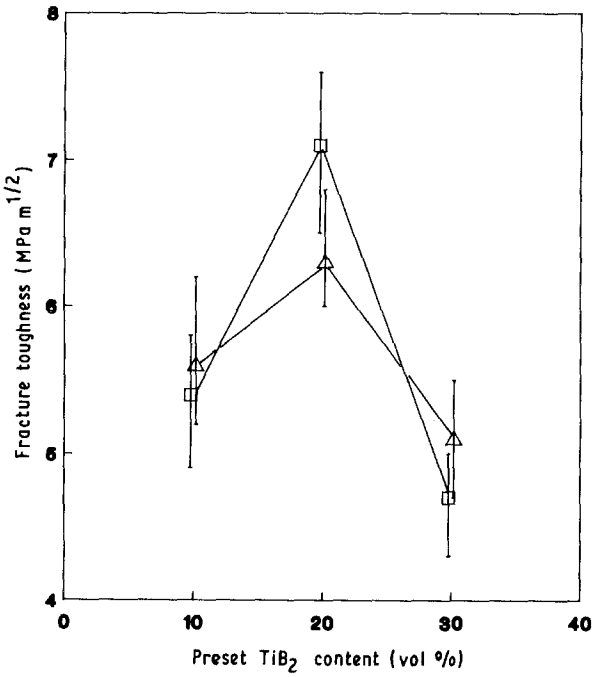

Figure 12 Fracture toughness of the composites as a function of the preset TiB_2 content. The composites were obtained through the following pressureless-sintering procedures: (i) preheating at 1300 °C for 30 min and then sintering at 1500 °C for 4 h in vacuum (△), (ii) preheating at 1300 °C for 3 h and then sintering at 1600 °C for 1 h in vacuum (□).

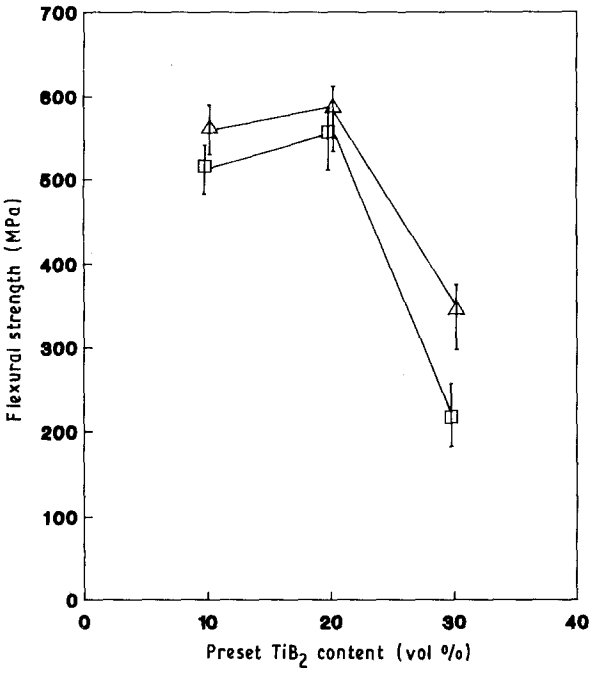

Figure 11 Dependence of the flexural strength of the composites on the preset TiB_2 content. The composites were obtained through preheating at 1300 °C for (□) 2 or (△) 3 h and then pressureless sintering at 1600 °C for 1 h in vacuum.

TiB_2, the flexural strength decreased markedly due to the low relative density as shown in Fig. 6.

Fig. 12 shows the fracture toughness of the composites as a function of TiB_2 content. These composites were obtained through the following sintering procedures.

(i) Preheating at 1300 °C for 30 min and then pressureless sintering at 1500 °C for 4 h in vacuum.

(ii) Preheating at 1300 °C for 3 h and then pressureless sintering at 1600 °C for 1 h in vacuum.

By using sintering procedure (ii), the composite containing 20 vol % TiB_2 gives a fracture toughness of 7.2 MPa $m^{1/2}$, slightly higher than that sintered by using procedure (i).

The higher flexural strength and fracture toughness in the composites sintered at 1600 °C for 1 h, compared with those sintered at 1500 °C for 4 h, may be due to the inhibited grain growth of Al_2O_3 and the less coalescence of TiB_2 particles, as discussed in Section 3.3.

4. Conclusions

In order to obtain Al_2O_3/TiB_2 composite through *in situ* reaction between TiO_2, boron and carbon, hot-pressing and pressureless-sintering processes have been studied. The conclusions are as follows.

1. In hot-pressing, in addition to TiB_2 and TiC, Al_2TiO_5 was found to be the main phase in the Al_2O_3 matrix.

2. In pressureless sintering, the Al_2O_3/TiB_2 composite can be successfully developed and densified up to > 99% relative density through the following firing procedures:

(i) preheating at 1300 °C for 30 min and then sintering at 1500 °C for ⩾ 3 h in vacuum.

(ii) Preheating at 1300 °C for ⩾ 3 h and then sintering at 1600 °C for 1 h in vacuum.

3. The Al_2O_3/20 vol % TiB_2 composite, which shows the best performance in the mechanical test, was obtained through preheating at 1300 °C for 3 h and sintering at 1600 °C for 1 h in vacuum. A flexural

strength of 580 MPa and a fracture toughness of 7.2 MPa $m^{1/2}$ was observed in this pressureless-sintered composite.

Acknowledgement

Funding support by the Ministry of Economic Affairs, Taiwan, is gratefully acknowledged. We also thank Mr Chun-Shoo Lee for his assistance in TEM observations.

References

1. P. F. BECHER and G. C. WEI, *J. Amer. Ceram. Soc.* **67** (1984) c-259.
2. K. NIIHARA and A. NAKAHIRA, in "Proceedings of the Third International Symposium on Ceramic Materials and Components for Engines", Las Vegas, November 1988, edited by V. T. Tennery (American Ceramic Society, Ohio, 1988) p. 919.
3. M. FURUKAW, O. NAKANO and Y. TAKASHIMA, *Int. J. Refract. Hard Metals* **7** (1988) 37.
4. N. TAKAHASHI, Y. IYORI and H. HARA, *Hitachi Kinzoku Giho* **1** (1985) 41.
5. YU. I. KRYLOV, *Izv. Akad. Nauk SSSR Neorg. Mater.* **12** (1976) 1684.
6. G. V. SAMSONON and I. M. VINITSKII, "Handbook of Refractory Compounds" (IFI/Plenum, New York, 1980) p. 40.
7. M. W. CHASE Jr, C. A. DAVIES, J. R. DOWNEY Jr, D. J. FRURIP, R. A. MacDONALD and A. N. SYVERUD, in "JANAF Thermochemical Tables", 3rd Edn, Part II (American Chemical Society and the American Institute of Physics for the National Bureau of Standards, New York, 1985) pp. 274, 640.
8. S. G. SAMDANI, M. N. CHARY and A. ALI, *Trans. Ind. Ceram. Soc.* **29** (1970) 109.

Received 28 October
and accepted 16 December 1991